Ligand design and synthesis of new imidazo[5,1-*b*]quinazoline derivatives as α₁-adrenoceptor agonists and antagonists

Mohamed A. H. Ismail,[a,*] Mohamed N. Y. Aboul-Enein,[b]
Khaled A. M. Abouzid[a] and Rabah A. T. Serya[a]

[a]*Department of Pharmaceutical Chemistry, Faculty of Pharmacy, Ain Shams University, Cairo, Egypt*
[b]*National Research Center, Pharmaceutical Chemistry Branch, Dokki, Cairo, Egypt*

Abstract—A series of new imidazo[5,1-*b*]quinazoline derivatives (**VII–IX**) was designed, synthesized, and biologically evaluated for their in vivo hypotensive or hypertensive activities. The design of these compounds was based upon the molecular modeling simulation of the fitting values and conformational energy values of the best-fitted conformers to both the α₁-adrenoceptor (α₁-AR) agonist and α₁-adrenoceptor (α₁-AR) antagonist hypotheses. These hypotheses were generated from their corresponding lead compounds using CATALYST software. The simulation studies predicted that compounds **IX**a and **IX**e would have probable affinity for the α₁-AR antagonist hypothesis, while compounds **IX**b, **IX**c, and **IX**g predicted a higher affinity for the α₁-AR agonist hypothesis. In vivo biological evaluation of these compounds for their effects on the blood pressure of normotensive cats was consistent with the results of molecular modeling studies, where compounds **IX**a and **IX**e exhibited hypotensive activity, while compounds **IX**b, **IX**c, and **IX**g resulted in increasing the blood pressure of the experimental animals at different doses.
© 2005 Elsevier Ltd. All rights reserved.

1. Introduction

The α₁ adrenergic receptors α₁-ARs are a family of G-protein coupled seven-transmembrane helix receptors, which are mainly involved in the cardiovascular and central nervous system.[1] Like other adrenergic receptors, α₁-ARs are activated by catecholamines, adrenaline and noradrenaline. The α₁-ARs have divergent affinities for many synthetic drugs, which interact selectively as agonist or antagonists. Ligands acting as antagonists at the α₁-ARs subtypes have been used in the treatment of a variety of diseases including hypertension, asthma, and prostatic hypertrophy by relaxation of vascular smooth muscles containing a high concentration of α₁-AR.[2–4] Whereas, ligands acting as α₁-AR receptor agonists would exert vasoconstriction on vascular smooth muscles containing a high concentration of α₁-AR, leading to increased blood pressure.[4]

In this investigation, ligand design based on molecular modeling studies for the development of new ligands

acting as α₁-agonists or α₁-antagonists and their synthesis are performed herein.

It is well-known that both agonists and antagonist molecules possess structural features that would enable the formation of a strong drug–receptor complex (strong affinity).[5,6] But, the agonist possesses the ability to cause a stimulant action by its rapid rates of association and dissociation with the receptors, which will lead to production of numerous impulses needed to exert the activity (i.e., have intrinsic activity). With regard to the antagonists, they should bind more firmly to the receptors than the agonist and as a result they would have a higher rate of association and a lower rate of dissociation with the same receptors, resulting in cessation of impulses (i.e., high affinity and low or zero intrinsic activity).[5,6]

In 2000, Bremner et al.[7] reviewed that the α₁-ARs were recognized to comprise of α₁A,[8] α₁B,[8] α₁D,[8] and α₁L[9] subtypes, and ligands showing high binding selectivity, as antagonists, for these subtypes are available[2,7] and were reported to have three features, namely; (i) A basic nitrogen that is accessible and can easily be protonated at physiological pH; (ii) An aromatic ring; (iii) A preferably nonaromatic ring. But, the difference between these

subtypes was in the distances and angles between features of their pharmacophore (Hypotheses) generated by means of Catalyst softwares.[7] However, in 2002, Barbaro et al.[9] have excluded the above three features for the α_1-AR subtypes and proved that the typical pharmacophore (hypothesis) for the α_1-antagonist of antihypertensive lead drugs consists of five constraint features, namely: (i) one positive ionizable portion, (ii) one hydrogen bond acceptor, and (iii) three hydrophobic features. It seems that the five features would be more convenient than the three features for the ligands to be firmly bound to the receptor as antagonists. The later authors[9] have also reported that such a constraint pharmacophore was a valid one because it showed a good statistical significance and successfully predicted the affinity of molecules of, and external to, the training set used in that research and it has a significant correlation between the chemical structures of the studied compounds and their biological data. Moreover, it was also proved that the cardiovascular system involves all subtypes of α_1-ARs.[10] The current research comprises the generation of α_1-antagonist hypothesis based on the above-reported finding, to design new α_1-AR antagonist ligands.

Meanwhile, there were several attempts in the literature to develop a pharmacophore model of the α_1-adrenergic receptors for agonist ligands,[10] but no mention has been made of any specific structural requirements for the affinity to the various α_1-subtypes. It was stated[11] that the α_1-agonist binding pocket is located in the transmembrane domain near the extracellular face and that an aspartate side chain in the third transmembrane helix binds the hydrogen of the protonated amine of both agonists and antagonists. Close to this residue is also a large hydrophobic pocket containing conserved aromatic (hydrophobic) and serine/cysteine (H-bonding acceptor) residues. This means that the α_1-AR agonist hypothesis consists of only three features and hence their ligands will be less firmly held to it than with the antagonist.

In the current research, the hypotheses generations were performed by running the common features hypotheses generation method of Catalyst softwares. This method is applicable when the three-dimensional structure of the receptor is unknown and a series of compounds has been identified that have similar activity but dissimilar and/or flexible structures. The main idea of this approach is to identify hypotheses, which are templates derived from the structures of these compounds and representing the geometry of the receptor sites as a collection of function groups in three-dimensional space. The program gives 10 of these hypotheses as a result of an experimental by default. Thus, the α_1-AR antagonist hypotheses were generated from the corresponding α_1-AR antagonist antihypertensive lead compounds (1–15),[12,13] and the ideal hypothesis among the generated hypotheses was found to be number 10, because it contained the reported five crucial constraint features for selective α_1-antagonists[9] and it had more consistent simulation fitting values (to the respective ligands and training set compounds) with the experimental results than with other hypotheses.

Similarly, an ideal α_1-AR agonist hypothesis derived from α_1-agonist lead compounds (16–23)[14–17] was also generated by the default running of common features hypotheses generation method. The ranked hypothesis number 1 was found to be the ideal one because of its fitting values with the corresponding ligands and the training set compounds were more matched with the experimental results than other hypotheses.

The generated α_1-AR agonist and antagonist hypotheses were subjected to simulation compare/fit studies (using the best-fit algorithmic method) with the conformational model of the proposed training set compounds to predict their α_1-AR agonist or α_1-AR antagonist activities. The simulated fitting values of the best-fitted conformer may be a guide for prioritizing relative affinities of these compounds with their receptors.[11] Moreover, it has been reported that the conformational energies of a training set molecules must be taken into account in the design of new ligands from a template structure. It was found that the affinity of a ligand decreases when the conformational energy required to adopt a bioactive conformation (the conformational energy penalty) increases. This means that, as the conformational energy of a specific conformer increases, the energy required for a ligand to bind with its receptor increases too, and hence the affinity will be decreased.[18] A representative example of such statement in the literature[19] was that reported to compare between the conformational energies of some dopamine D_2 agonist compounds versus their agonist activity. It was found that highly active compounds would have conformational energies of less than 2 kJ mol^{-1}, whereas the moderately active compounds would display conformational energies of $8–10 \text{ kJ mol}^{-1}$, while the inactive compounds demonstrated conformational energies of 20 kJ mol^{-1}. Thus, the design of new ligands in this investigation would not only depend upon the compare/fit values, but also depend on the conformational energies of the best-fitted conformers of the training set compounds.

Literature surveys have been demonstrated that various imidazoquinazoline derivatives have wide diverse biological activities, including the anti-hypertensive activities through a selective α_1-antagonistic mechanism.[20–22] It was, also, reported that the arylpiperazinyl alkyl moiety was the key element in defining α_1-antagonist activity.[23–27]

Accordingly, new series of various substituted imidazo[5,1-*b*]quinazolines linked to arylpiperazine ring systems designed. The molecular simulation studies of these compounds revealed that some of these compounds have shown high fitting affinity with lower conformational energies with α_1-agonist hypothesis, while others have high fitting affinity and low conformational energies with the α_1-antagonist hypothesis, when compared to the respective lead compounds. In view of these observations, we were motivated to synthesize these molecules and examine their effects on the normotensive blood pressure of anesthetized cats, hoping that they would develop new α_1-agonist and α_1-antagonist ligands. The sequence of the reactions, followed in the synthesis of the titled compounds, is shown in Scheme 1.
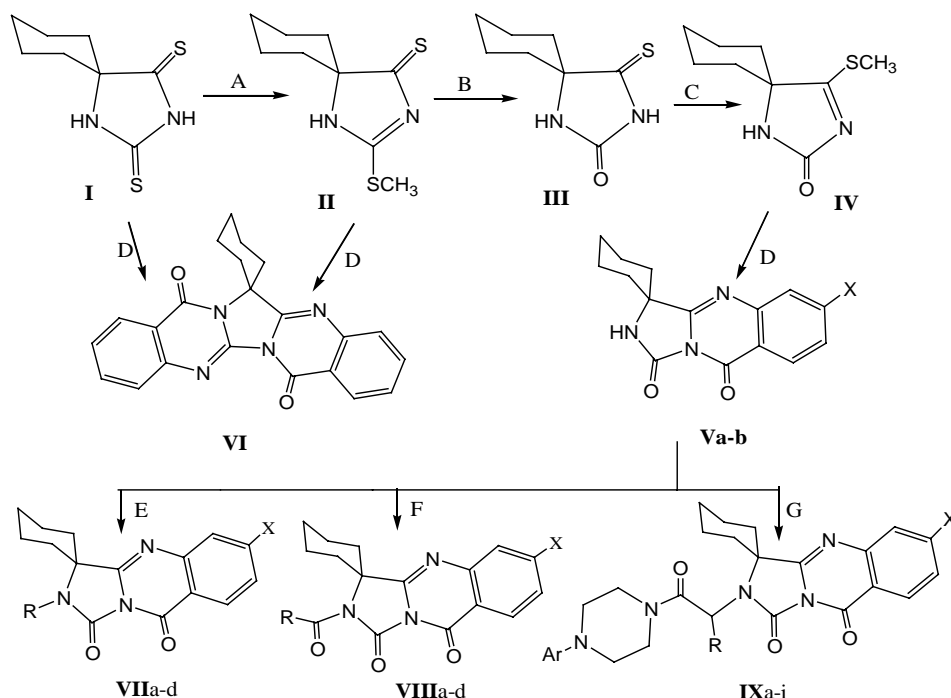
Scheme 1. Compounds: **Va**, X = H; **Vb**, X = Cl; **VIIa**, R = C$_2$H$_5$, X = H; **VIIb**, R = C$_6$H$_5$CH$_2$, X = H; **VIIc**, R = C$_2$H$_5$, X = Cl; **VIId**, R = C$_6$H$_5$CH$_2$, X = Cl; **VIIIa**, R = CH$_3$, X = H; **VIIIb**, R = C$_2$H$_5$, X = H; **VIIIc**, R = C$_6$H$_5$, X = H; **VIIId**, R = C$_6$H$_5$, X = Cl; **IXa**, Ar = C$_6$H$_5$, R = H, X = H; **IXb**, Ar = 4-FC$_6$H$_4$, R = H, X = Cl; **IXc**, Ar = 2-(CH$_3$O)C$_6$H$_4$, R = H, X = H; **IXd**, Ar = 2-F-C$_6$H$_4$, R = H, X = H; **IXe**, Ar = C$_6$H$_5$, R = H, X = Cl; **IXf**, Ar = 2-F-C$_6$H$_4$, R = H, X = Cl; **IXg**, Ar = 2(–CH$_3$O)C$_6$H$_4$, R = H, X = Cl; **IXh**, Ar = C$_6$H$_5$, R = CH$_3$, X = H; **IXi**, Ar = C$_6$H$_5$, R = CH$_3$, X = Cl. Reagents: A = 8% NaOH, (CH$_3$)$_2$SO$_4$; B = HCl (20%); C = CH$_3$-I, K$_2$CO$_3$; D = anthranilic acid or 4-chloroanthranilic acid; E = R-X, K$_2$CO$_3$, acetone; F = acetic anhydride, propionic anhydride; or benzoyl chloride, G = 4-aryl-1-chloroacetyl-piperazine or 4-aryl-1-(2-chloropropionyl)-piperazine.

2. Results

2.1. Synthesis of the imidazo[5,1-*b*] quinazoline derivatives (VIIa–b, VIIIa–d, and IXa–i)

The synthesis of the designed imidazo[5,1-*b*]quinazolines (Scheme 1) was carried out starting from the dithiohydantoin (**I**)[28] via its S-methylation at position 2 into **II**,[29] followed by the removal of CH$_3$-SH, and then S-methylation of the separated mono-thione (**III**)[29] into 4-mercaptomethylimidazoline (**IV**).[30] The latter intermediate was then condensed with anthranilic acid or 4-chloroanthranilic acid to produce the key imidazolo[5,1-*b*]quinazoline intermediates (**Va,b**). Fusion of the anthranilic acid with **I** or **II** generated the dimeric condensation product (**VI**). The reaction of **Va,b** with different alkyl halides, acid chlorides, and 4-arylpiperazinyl-oxoalkyl chlorides afforded the corresponding targeted derivatives (**VIIa–d**, **VIIIa–d**, and **IXa–i**). Structural confirmation of new compounds was forthcoming from IR, NMR, MS, and Elemental Microanalysis data.

2.2. Generation of α$_1$-AR antagonist hypothesis

The lead compounds, which were reported to have selective α$_1$-AR antagonistic activity (Fig. 1), namely; Prazosin (**1**),[25] Doxazosin (**2**),[26] WB 4101 (**3**)[7], Cmd-1 (**4**),[1] SNAP5089 (**5**),[7] and other reported imidazoquinazolines, imidazobenzo-thiadiazine derivatives linked to aryl piperazines (**6–15**),[7,23] were used to generate common feature hypotheses of the α$_1$-AR antagonists.

The set of conformational models of each structure of the lead compounds was performed and was used to generate the common feature hypotheses (by default), where 10 hypotheses were generated. The assessment of the ideal hypothesis among the generated ones indicated that hypothesis ranked number 10 was the ideal one (Figs. 2 and 3). This is because the simulated fitting values of such a hypothesis with the training hypotensive test set compounds (**IXa** and **IXe**) (Figs. 4 and 5) were more consistent with the experimental results than with the hypothesis numbers 1–9. Thus, hypothesis number 10 showed high fit values (2.98 and 2.99, respectively), with corresponding low conformational energies (0.24 and 0.07 kcal mol^{-1}), with those two test compounds. Whereas, the fitting values of the same two compounds with hypothesis numbers 1–9 were below 1.95 with high conformational energies exceeding 14.89 kcal mol^{-1}.

Such an ideal hypothesis encompassed five features namely; positive ionizable (PI), hydrogen bonding acceptor (HBA), and three hydrophobic features (HY1, HY2, and HY3) (Figs. 2 and 3). As mentioned before, the reported α$_1$-AR antagonist hypothesis by Barbora et al[9] contains the same kind and number of features like our hypothesis. Nevertheless, the difference between them was in the constraint distances between the five features (Table 1 and Fig. 2). Meanwhile, the constraint angles between features of the reported hypothesis were not mentioned, but herein we report the range of constraint angles between features of our hypothesis, as shown in Table 1 and Figure 3.
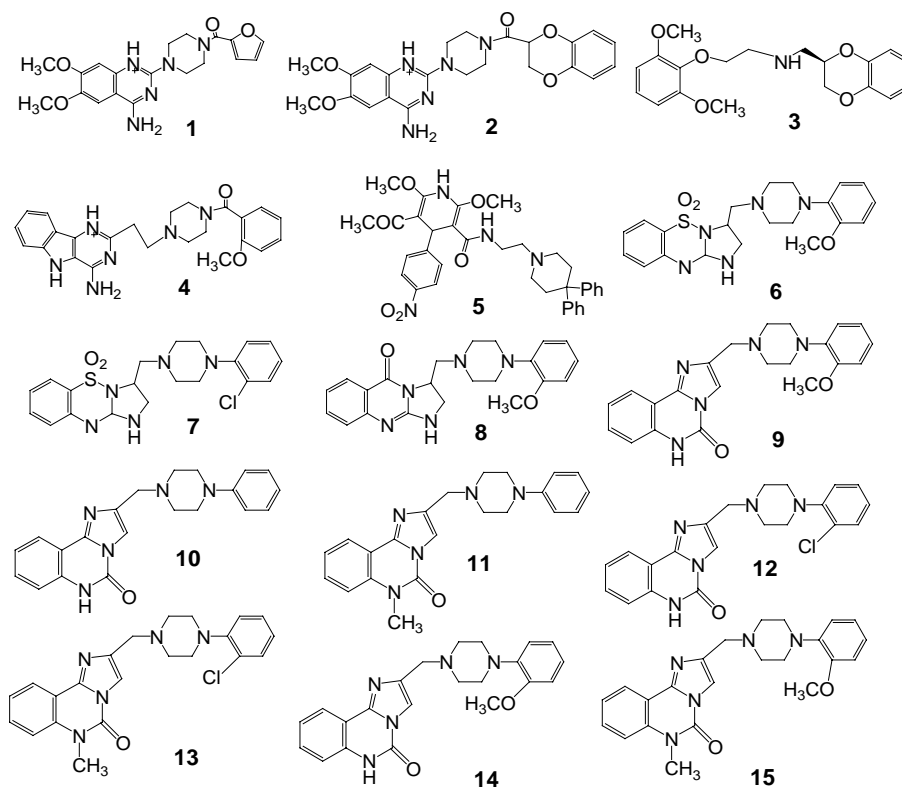
Figure 1. Structures of α₁-AR antagonists lead compounds used for the generation of α₁-AR antagonist hypothesis.
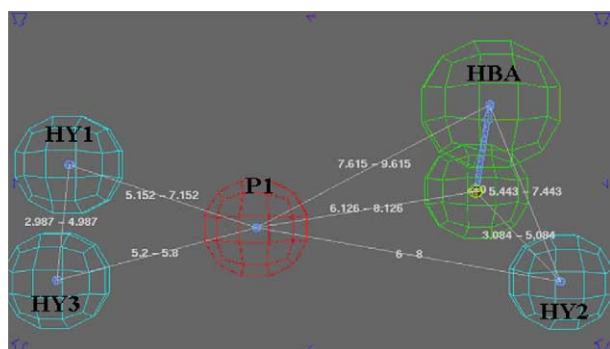

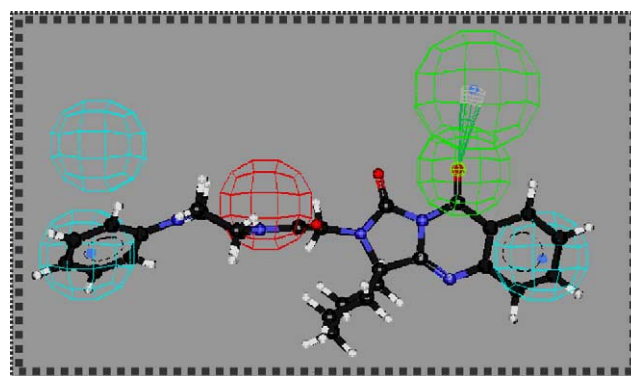**Figure 2.** Constraint distances of α₁-AR antagonist hypothesis.

Figure 3. Constraint angles of α₁-AR antagonist hypothesis.

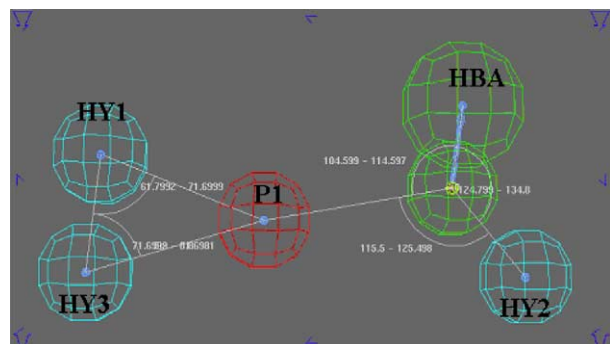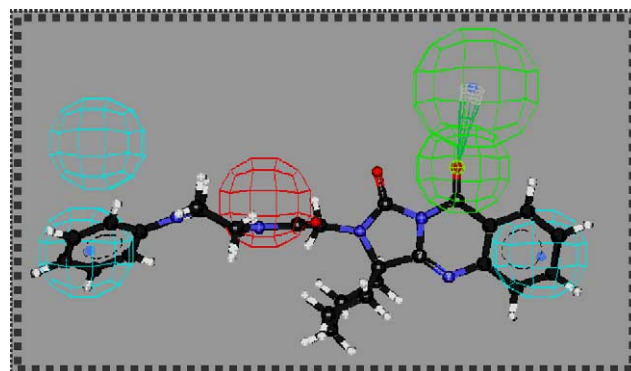**Figure 4.** Mapping of α₁-AR antagonist hypothesis and **IX**a.

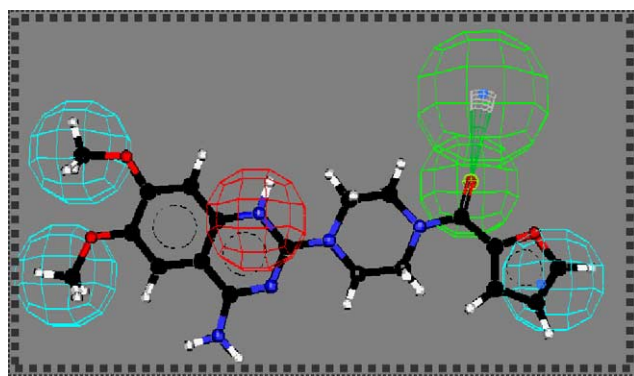**Figure 5.** Mapping of α₁-AR antagonist hypothesis and **IX**e.

Table 1. Comparison of the constraint distances and angles between the features of the reported Barbaro's α_1-AR antagonist hypothesis and the features of our hypothesis measured by Catalyst visualizer

Dimensions	Barbaro's hypothesis	Our hypothesis(values are recorded in ranges)
Constraint distances (Å) between features of Barbaro's and our hypotheses	PI-HBA, 5.62; PI-HY1, 6.69; PI-HY2, 6.17; PI-HY3, 9.78	PI-HBA, 6.126–8.126; PI-HY1, 5.152–7.192; PI-HY2, 5.200–5.800; PI-HY3, 6.00–8.000
Constraint angles (°) between features of Barbaro's and our hypotheses	Not reported	PI-HBA-HY3, 115.500–125.498; HY3-HBA vector, 124.799–134.800; PI-HBA vector, 104.599–114.597; PI-HY1-HY2, 61.7992–7106999; PI-HY2-HY1, 71.6989–80.86981

Abbreviation used: PI, positive ionizable feature; HBA, hydrogen bond acceptor feature; HBA vector, direction of the hydrogen bond acceptor vector; HY, hydrophobic feature.

Further validation of this ideal α_1-AR antagonist hypothesis was assessed through the following:

(a) This hypothesis showed full mapping of all of its five features with the lead structure of the Prazosin® (**1**) (the most active α_1-AR antagonist), with a low conformational energy = 1.96 kcal mol^{-1}, which means absence of any steric clashes. Such an advantage was not present in the mapping of the reported Barbaro's hypothesis[9] with the same lead compound, where it was reported to show full mapping with only four features, while the 5th feature (HY3) performed partial mapping with high steric clashes (Fig. 6).

(b) The database search study for examining the affinity of such an antagonist hypothesis with the molecular structures of the provided databases with Catalyst 4.8, namely NCI 2000, Maybridge 2001, and MiniMaybridge, which contain 296092 compounds, revealed that only 663 molecules ($\sim$0.22% of the total), have been retrieved from the databases (Table 2). Such a low percentage of the recognized database molecules by our hypothesis, in comparison to that with Barbara's hypothesis (reported $\sim$0.27%), may give an additional advantage to our hypothesis.

Figure 6. Mapping of α_1-AR antagonist hypothesis and Prazosin®.

In addition, the retrieved (mapped) hit molecules by our hypothesis were investigated and some of the recognized known α_1-AR antagonist agents, among these hits, were distinguished to have high fitting values with low conformational energies. For example: the known α_1-AR antagonist agents; Etoperidone (**16**)[1,31] (NCI Code No.: 304398), Ergotamine (**17**)[1,32] (NCI Code No.: 41869), isobutyl analogue of Ergotamine (**18**)[32] (NCI Code No.: 122047), and chlorimipiphinine (**19**)[33] (NCI Code No.: 113426) (Fig. 7), which were well-known to interact with the adrenergic receptors as antagonists, were among the mapped database hits by our hypothesis. Interestingly, such mapping of those α_1-AR antagonists was found to have high fitting values (3.98, 3.5, 4.2, and 3.6, respectively) with the corresponding low conformational energies (3.11, 0.60, 3.60, and 2.69 kcal mol^{-1}).

2.3. Generation of α_1-AR agonist hypothesis

The generation of common feature hypotheses of the α_1-AR agonist was obtained by adopting the same steps to construct the α_1-AR antagonist hypotheses, but by using a set of conformational models of each structure of the reported selective α_1-agonistic lead compounds,[14–17,34] namely; Phenylephrine (**20**),[14] Proametine (**21**),[15] SDZ-NVI 085 (**22**),[16] SKF1-89748 (**23**),[16] Heptaminol (**24**),[17] ST587 (**25**),[17] Octahydrobenzo-[g]quinoline (**26**),[34] and (S)-diaza-spiro[1,3]cyclopent-1-ene)-5,2'-(7'-methyl-tetrahydronaphthalene (**27**)[34] (Fig. 8).

The common feature hypotheses generation gave 10 hypotheses. The assessment of the generated α_1-AR agonist hypotheses revealed that hypothesis ranking number 1 (Figs. 9 and 10) was proved to be the ideal one rather than the other generated hypothesis numbers 2–10. This was because hypothesis number 1 has more matched simulation data with experimental biological activity. Thus, the fitting affinity of the hypertensive agents among the training set molecules in this research (**IX**b, **IX**c, and **IX**g) (Figs. 11–13), with hypothesis number 1, showed high fit values (2.78, 2.80, and 2.82,

Table 2. Mapping of Catalyst database molecules with α_1-AR antagonist hypothesis

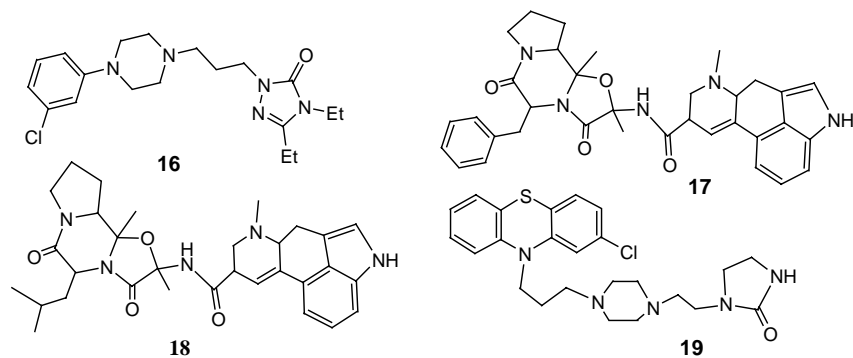| Database	Total numbers of molecules	Number of retrieved (mapped) hits	% of retrieved (mapped) hits
NCI 2000	238819	539	0.223
Maybridge2001	55273	124	0.22
MiniMaycridge	2000	0	0.0
Total	296092	663	0.222

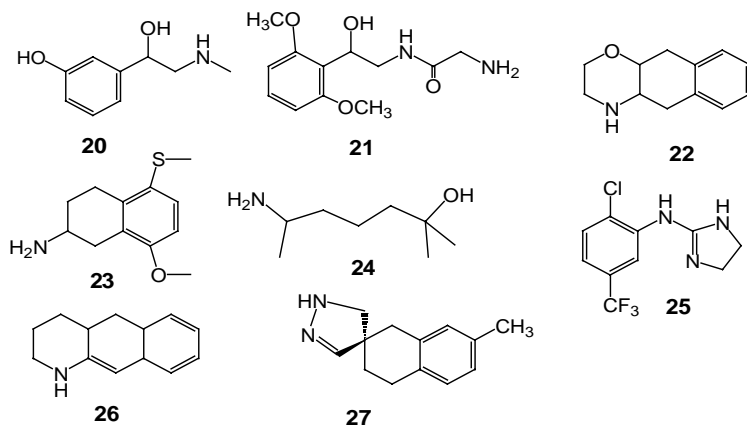**Figure 7.** Known α$_1$-AR antagonists in the database, which are mapped by our α1-AR antagonist hypothesis.

Figure 8. Structures of α$_1$-AR agonist lead compounds used for the generation of α$_1$-AR agonist hypothesis.
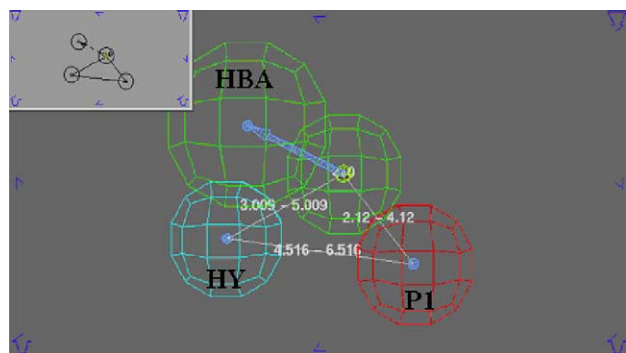

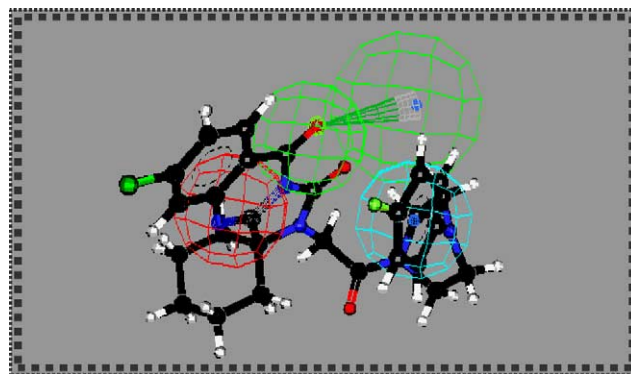**Figure 9.** Constraint distances of of α$_1$-AR agonist hypothesis.

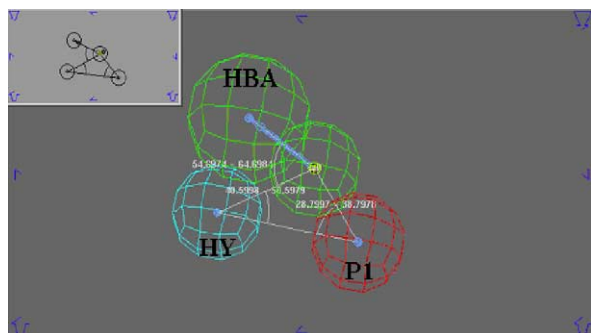**Figure 11.** Mapping of α$_1$-agonist hypothesis and **IX**b.

Figure 10. Constraint angles of of α$_1$-AR agonist hypothesis.
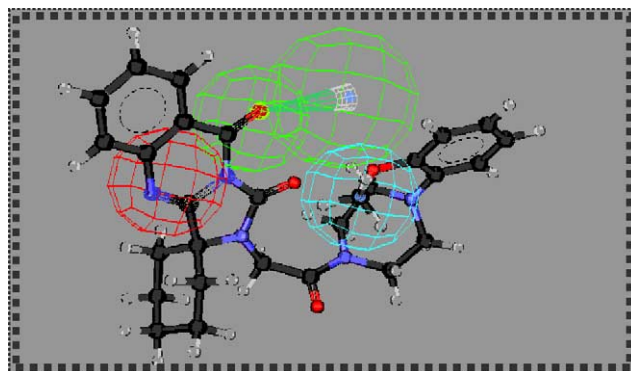

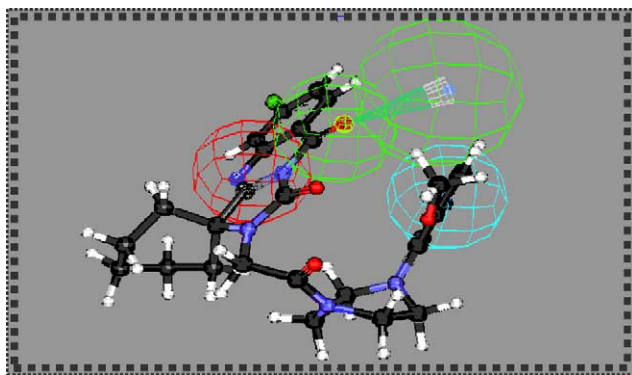**Figure 12.** Mapping of α$_1$-agonist hypothesis and **IX**c.

Figure 13. Mapping of α₁-agonist hypothesis and **IX**g.

respectively) with corresponding low conformational energies (0.67, 5.9, and 5.99 kcal mol^{-1}). However, hypotheses ranked numbers 2–9 showed mapping with the same hypertensive training set molecules with lower fit values (<2.10) through high conformational energies (>14.99) kcal mol^{-1}.

This ideal α₁-AR agonist hypothesis contains three features namely; positive ionizable (PI), hydrogen bonding acceptor (HBA), and only one hydrophobic feature (HY) (Figs. 9 and 10). It was concluded that the reported α₁-AR agonist hypothesis by Guimares and Daniel[10] has these three features, but, there seems to be no mention of any dimensions between them. Herein, we report, for the first time, the constraint dimensions between the three features in our generated α₁-AR agonist hypothesis (Table 3 and Figs. 9 and 10).

Additional validation of such an α₁-AR agonist hypothesis was achieved by the following:

(a) It demonstrated a full mapping of all its features to the molecular structure of phenylephrine (the most active α₁-AR agonist), through a low-energy conformation (0.07 kcal mol^{-1}) (see Fig. 14).
(b) Furthermore, a database search study for examin-

ing the affinity of this agonist hypothesis with the molecular structures of the provided Catalyst databases was carried out. Nevertheless, the results showed that 13.8% of the database molecules were recognized by this hypothesis, as shown in Table 4.

As expected, the high percentage of the mapped molecules, in such a hypothesis, could be due to it having only three features, which increases the probability of retrieving a large number of database molecules, even if they are not selectively bound to the (α₁-AR) receptor as agonists. Nevertheless, searching for sympathomimetic adrenergic agents, in the mapped NCI hits, has revealed that epinephrine (**28**) (NCI Code No.:62786), norepinephrine (**29**) (NCI Code No.: 7930), (−) ephedrine (**30**) (NCI Code No.: 8871), norephedrine (**31**) (NCI Code No.: 17704), and isoprenaline (**32**) (NCI Code No.: 9975) (Fig. 15) showed high fitting affinities (2.99 for all), with explicitly low conformational energies (2.5, 0.07, 6.15, 1.6, and 2.18 kcal mol^{-1}, respectively).

2.4. Comparison between α₁-AR antagonist and α₁-AR agonist hypotheses

The comparison between the α₁-AR antagonist and α₁-AR agonist hypotheses has revealed that there were three shared binding features between the two hypotheses namely: positive ionizable, H-bond acceptor, and one hydrophobic region. It therefore appears that the α₁-AR antagonist hypothesis makes use of the two additional points of attachment not used by the agonists, which are the remaining two hydrophobic features in the antagonist hypothesis. These two additional hydrophobic pockets are essential to make a firm binding with the receptors that are essential for the antagonistic activity.

Table 3. Constraint features dimensions of the (α₁-AR) agonist hypothesis measured by Catalyst Visualizer

Average angles (°) between features	Average distances (Å) between features
HY–HBA vector, 54.6974–64.6984	HBA–PI, 2.120–4.120
HBA–PI–HY, 28.7997–38.7978	PI–HY, 4.516–6.516
PI–HY–HBA, 40.5998–50.979	HY–HBA, 3.009–5.009

Abbreviation used: PI, positive ionizable feature; HBA, hydrogen bond acceptor feature; HBA vector, direction of the hydrogen bond acceptor vector; HY, hydrophobic point feature.

Figure 14. Mapping of α₁-agonist hypothesis and Phenylephrin.

Table 4. Mapping of Catalyst database molecules with (α₁-AR) agonist hypothesis

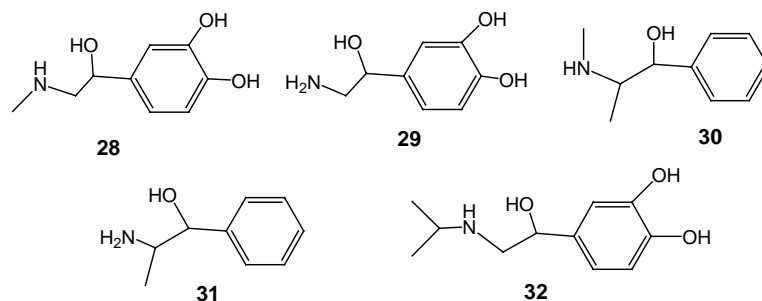| Database	Total numbers of molecules	Number of the retrieved (mapped) hits	% of retrieved (mapped) hits
NCI 2000	238819	34940	14.63
Maybridge2001	55273	5692	10.30
MiniMaybridge	2000	193	9.65
Total	296092	40825	13.80

Figure 15. Known sympathomimetic agonists in the database, which are mapped by our α_1-AR agonist hypothesis.

2.4.1. Molecular modeling simulation studies of the training set of imidazo[1,5-b]quinazolines. The training set structures of the titled imidazo[1,5-b]quinazoline derivatives (**V**a,b, **VII**a–d, **VIII**a–d, and **IX**a–i) were belt separately, using Catalyst softwares. Then, the conformational models of each structure were performed (in the range of 20 kcal mol^{-1}), to find all possible conformations of each structure and their conformational energies. Molecular modeling simulation studies were then conducted by measuring the compare/fit values, separately, between the conformational models of the training set molecules and the ideal α_1-AR antagonist and the ideal α_1-AR agonist hypotheses. The results of the best fitting values, as well as the conformational energy of the best-fitted conformer with both hypotheses, are given in Table 5. The results of such simulation studies have revealed that compounds **IX**a, **IX**b, **IX**c, **IX**e, and **IX**g would be promising active hit molecules.

3. In vivo biological evaluation

The promising active hit molecules of the imidazo[1,5-b]quinazolines containing the arylpiperazinyloxoalkyl moieties (**IX**a, **IX**b, **IX**c, **IX**e, and **IX**g), as well as the corresponding benzyl and acyl analogues (**VI**b and **VIII**a), were subjected to an in vivo biological evaluation of their

effects on the arterial blood pressure of normotensive adult cats, adopting the reported method,[35] which were used in our laboratory in previous publications.[36]

3.1. Results of in vivo biological studies

Table 6 shows the effect of the minimum effective molar doses of the training set compounds on the systolic and diastolic arterial blood of anesthetized normotensive adult cats compared to control and reference drug (prazosin). The study has revealed that only two compounds among the promising hit molecules (namely: **IX**a and **IX**e) exerted effective hypotensive activities at different doses. On the contrary, the other hit compounds, **IX**b, **IX**c, and **IX**g showed explicit hypertensive activities for both systolic and diastolic pressures at different doses. These results have indicated that compounds **IX**a and **IX**e preferentially act as α_1-AR antagonist ligands, while the other hit molecules: **IX**b, **IX**c, and **IX**g act as α_1-AR agonist ligands.

3.2. Correlation of the simulation molecular affinities and the experimental biological evaluation data

The experimental biological evaluation data revealed that compounds **IX**a and **IX**e have significant hypotensive activity, while compounds **IX**b, **IX**c, and **IX**g exert

Table 5. Compare/fit and conformational energy values of the best fitted conformers of the imidazo[1,5-b]quinazolines and the α_1-AR antagonist and agonist hypotheses

Compounds	Numbers of conformers	Fitting values with α_1-antagonist hypothesis	Conf. energy at the antagonist hypothesis (kcal mol^{-1})	Fitting values with α_1-AR agonist hypothesis	Conf. energy at the agonist hypothesis (kcal mol^{-1})
Vb	5	No mapping	—	No mapping	—
Vd	5	No mapping	—	No mapping	—
VIIa	9	1.4	8.7	2.0	9.8
VIIb	15	1.5	2.28	2.01	12.3
VIIc	8	1.9	11.25	2.18	11.3
VIId	11	1.7	6.5	2.03	10.53
VIIIa	7	−0.27	15.54	1.97	9.11
VIIIb	10	1.8	11.9	1.7	16.98
VIIIc	6	2.0	7.5	1.99	9.91
VIIId	5	1.6	7.68	2.12	11.3
IXa	105	**2.98**	**0.24**	**2.80**	13.18
IXb	88	**2.99**	**15.21**	**2.78**	**0.67**
IXc	142	**2.90**	**11.25**	**2.80**	**5.9**
IXd	103	1.81	18.25	1.89	15.9
IXe	71	**2.99**	**0.07**	2.70	12.08
IXg	49	**2.92**	**13.77**	**2.82**	**5.99**
IXh	61	2.6	12.22	2.12	17.3
IXi	55	2.51	11.2	2.11	12.93

Bold and underline indicates the important numbers which reflect the biological activity of the corresponding molecules.

Table 6. Effect of test compounds on systolic and diastolic blood pressure of anaesthetized normotensive cats

Compound	Dose (mmol/kg)	Systolic BP (mmHg) mean ± SE	Mean change %	Diastolic BP (mmHg) mean ± SE	Mean change %
Control	—	134.1±2.01	—	125.0 ± 1.35	—
Reference	0.00065	92.5 ± 2.21	−31	85.4 ± 1.55	−31
IXa	0.0007	**101.8±3.1**	**−24**	**93.75 ± 2.1**	**−25.0**
IXb	0.00063	**156.22 ± 1.2**	**+16.5**	**140.6 ± 4.5**	**+12.5**
IXc	0.00066	**155.6 ± 4.4**	**+16.5**	**139.37 ± 2.3**	**+11.5**
IXe	0.00065	**112.0 ± 1.2**	**−16.5**	**106.25 ± 4.1**	**−15.0**
IXg	0.00062	**150.86 ± 0.5**	**+12.5**	**135.0 ± 2.5**	**+8.10**
VIIb	0.00092	136.0 ± 1.99	—	127.6 ± 1.51	—
VIIIa	0.0007	133.0 ± 1.56	—	129.6 ± 2.89	—

Significantly different from respective control values at $p < 0.05$. Each value represents the means ± SE of six similar responses. Mean change with negative sign = the drug act as hypotensive, the positive sign = the drug act as hypertensive. Bold indicates the high values of the biological activity of the corresponding molecules.

potent hypertensive activity (Table 6). The molecular modeling simulation studies have indicated that the compare/fitting values for compounds **IXa**, **IXb**, **IXc**, **IXe**, and **IXg** with both the α_1-AR agonist and α_1-AR antagonist hypotheses had high fitting values (Table 5). Ambiguity that compounds **IXa** and **IXe** had hypotensive activity, while compounds **IXb**, **IXc**, and **IXg** had hypertensive effects though they have the same heterocyclic skeleton, was overcome by considering not only the fitting values, but also the conformational energies of the best-fitted conformers. These two values could be considered as good tools for the design of new ligands by molecular simulation. One of the most important advantages of Catalyst programs is that it can automatically measure these two values.

3.3. Structural activity relationship (SAR) of the α_1-AR agonist and antagonist leads of the prepared imidazo[5,1-*b*]quinazoline derivatives (IXa-i)
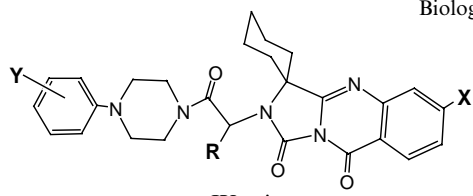
The data in Table 7 have indicated that the SAR for α_1-AR antagonist (hypotensive) activity, among the prepared imidazo[5,1-*b*]quinazoline derivatives, included the absence of any substituents at the phenyl group of the arylpiperazine moiety and no branching at the oxoethyl linker; (e.g., **IXa** and **IXe**), while the (α_1-AR) agonist (hypertensive) activity involved either *o*-methoxy or *p*-fluoro substituents at the phenyl ring of the arylpiperazine moiety and no branching at the oxoethyl linker (e.g., **IXb**, **IXc**, and **IXg**). Substitution of phenyl ring of the aryl piperazine moiety by a fluorine atom at the p-position (as in **IXd**, **IXf**), or branching the linker oxoethyl group by adding a methyl group (as in **IXh**, **IXi**), will abolish both the agonistic and antagonistic activities.

4. Conclusion

Comparing the conformational energies of the best fitted conformers to the α_1-AR agonist hypothesis and that of the best fitted conformer to the α_1-AR antagonist hypothesis for compounds **IXa**, **IXb**, **IXc**, **IXe** and **IXg** would disclose such a new approach for the ligand design of α_1-AR agonists and antagonists. The obtained data concluded that the conformation energies of the conformers that made best fitting for all the features in the α_1-AR antagonist hypothesis for compounds **IXa** and **IXe** were very low (0.24 and 0.07 kcal mol^{-1}, respectively). Such energies were much lower than conformational energies of the conformers that effected the best-fitting for all the features in the α_1-AR agonist hypothesis (13.18 and 12.08 kcal mol^{-1}, respectively). This finding

Table 7. SAR for the agonist and the antagonist activity of the prepared imidazo[5,1-*b*]quinazolines (**IXa–i**)

IXa -i

Compounds	Y	R	X	Biological activity on BP	Effects of (**IXa–i**) on systolic/diastolic BP
IXa	H	H	H	Hypotensive	−24.0%/−25.0%
IXe	H	H	Cl	Hypotensive	−16.5%/−15.0%
IXb	*p*-F	H	Cl	Hypertensive	+16.5%/+12.5%
IXc	*o*-(O-CH$_3$)	H	H	Hypertensive	+16.5%/+11.5%
IXg	*o*-(O-CH$_3$)	H	Cl	Hypertensive	+12.5%/+08.5%
IXd	*o*-F	H	H	No action	—
IXf	*o*-F	H	Cl	No action	—
IXh	H	CH$_3$	H	No action	—
IXi	H	CH$_3$	Cl	No action	—

proved that compounds **IX**a and **IX**e would be more stable when they acted as α_1-AR antagonists, and hence they would exhibit a hypotensive effect on the normotensive cats. On the other hand, the conformational energies of the conformers that made best fitting for all the features in the α_1-AR agonist hypothesis for compounds **IX**b, **IX**c, and **IX**g were low (5.9, 5.99, and 0.67 kcal mol^{-1}, respectively), and these energies were still much lower than those of the conformers that fitted all the features in the α_1-AR antagonist hypothesis (11.55, 13.77, and 15.21 kcal mol^{-1}, respectively). Accordingly, these molecules would be more stable when they bound to the α_1-AR agonist hypothesis, and hence they would elevate the blood pressure of the experimental animals.

5. Experimental

Melting points were determined with a Stuart Scientific apparatus and are uncorrected. FT-IR spectra were recorded on a Perkin-Elmer spectrophotometer and measured by v' cm^{-1} scale using KBr cell. ^{1}H NMR spectra were measured in δ scale on a JEOL 270 MHz spectrometer. Unless otherwise stated, the spectra were obtained on solutions in DMSO and referred to TMS. The electron impact (EI) mass spectra were recorded on Finnigan Mat SSQ 7000 (70 ev) mass spectrometer. The peak intensities, in parentheses, are expressed as percentage abundance. Analytical thin layer chromatography (TLC) was performed on Merk Kieselgel 60PF$_{254}$ silica on Aluminum backed sheets. All R_f values were recorded from the center of the spots. All Tlc solvent proportions were measured volume by volume. Column chromatography was performed using Merk Silica gel (mesh size = 0.032–0.064 mm). All reagents and solvents were purified and dried by standard techniques. Solvents were removed under reduced pressure in a rotary evaporator. Elemental microanalysis was performed at the Microanalytical Center, Ain-Shams University. The preparation of 2,4-dithioxo-1,3-diazaspiro[4,5]decane (**I**),[28] 2-methylthio-4-thioxo-1,3-diazaspiro[4,5]decan-2-ene (**II**),[29] 4-thioxo-1,3-diazaspiro[4,5]-decan-2-one (**III**),[29] 4-methylthio-1,3-diazaspiro[4,5]decan-3-ene-2-one (**IV**),[30] 4-aryl-1-(2-chloroacetyl)piperazines,[30] and 4-aryl-1-(2-chloropropionyl)piperazines[30] was performed, according to the reported procedures.

5.1. Preparation of 15,15-pentamethylene-6,7,13,14-tetrahydro-15(*H*)-diquinazolino[3,2-*a*; 3′,2′-*c*]imidazole-6,13-dione (V)

Method A: A mixture of 2,4-dithiohydantoin (**I**) (1.0 g, 5 mmol) and anthranilic acid (0.69g, 5 mmol) was heated at 100 °C in an oil bath for 3 h until the effervescence ceased. The solid product was triturated with ethanol and filtered. The precipitate was crystallized from DMSO/ethanol to give **V** as white crystals (1.3 g, 3.51 mmol, 70%), m.p. 350 °C. *Method B*: A mixture of 2-methylthio-4-thioxo-2-imidazoline (**II**) (1.07 g, 0.005 mol) and anthranilic acid (0.69 g, 5 mmol) was heated at 110 °C for 2 h. The reaction mixture was handled, as shown in *method A*, to produce compound **V** as white crystals (1.45 g, 3.91 mmol, 78.2%); m.p. 350 °C. (Found:

C, 71.58; H, 4.93; N, 15.46, $C_{22}H_{18}N_4O_2$ requires C, 71.35; H, 4.86; N, 15.13%.) MS (EI): *m/z* 370 (M$^+$, 100%).

5.2. Preparation of 3,3-pentamethylene-1,2,3,9-tetrahydro-imidazo[5,1-*b*] quin-azoline-1,9-diones (VIa,b)

General procedure: A mixture of 4-methylthio-imidazoline derivative (**IV**) (0.99 g, 5 mmol) and anthranilic acid (0.69 g, 5 mmol) for (**VI**a) or 4-chloroanthranilic (0.85 g, 5 mmol) for (**VI**b) was heated at 120 °C for (**VI**a) or at 150 °C for (**VI**b) in an oil bath for 3 h until the effervescence ceased. The solid product was triturated with ethanol filtered and the obtained precipitate was washed with ethanol, and crystallized from acetone.

5.2.1. For compound (VIa). It was separated as white crystals (0.6 g, 2.23 mmol, 44.5%), m.p. 290 °C. (Found: C, 66.51; H, 5.31; N, 15.49, $C_{15}H_{15}N_3O_2$ requires C, 66.91; H, 5.57; N, 15.61%.) MS (EI): *m/z* 269 (M$^+$, 74.08%). IR(FT): 3420(NH), 1635, 1582 (two CO). ^{1}H NMR; 1.59–1.9 (m, 10H, cyclohexyl), 7.5–8.1 (m, 4H, Ar–H), 9.3 (br, 1H, D^{2}O exchangeable, NH).

5.2.2. For compound (VIb). It was separated as faint yellowish white crystals (0.85 g, 2.8 mmol, 56%), m.p. 285 °C. (Found: C, 59.55; H, 4.57; N, 13.52 $C_{15}H_{14}ClN_3O_2$ requires C, 59.31; H, 4.65; N, 13.83%). MS (EI): *m/z* 303 (M$^+$, 100%), *m/z* 305 (M+2, 32.3%.) IR(FT): 3421(NH), 1686, 1632 (two CO). ^{1}H NMR; 1.7–1.9 (m, 10H, cyclohexyl), 7.5–8.22 (m, 4H, Ar–H), 9.7 (br, 1H, D^{2}O exchangeable, NH).

5.3. Preparation of 2-alkyl-3,3-pentamethylene-1,2,3,9-tetrahydroimidazo[5,1-*b*]quinazoline-1,9-diones (VIIa–d)

General procedure: To a mixture of (**7**a,b) (1.0 mmol) and K^{2}CO^3 (1 g) in dry acetone (30 ml), appropriate alkyl halide [viz.: ethyl iodide, benzyl chloride] (1.0 mmol) was added. The reaction mixture was refluxed for 24 h and then filtered off. The solvent was evaporated under vacuum and the residue was triturated with ether. The formed solid was crystallized from acetone–ether to produce the titled compounds (**VII**a–d).

5.3.1. For compound VIIa. It was separated as white crystals (88% yield), m.p. 160 °C. (Found: C, 68.21; H, 6.25; N, 13.98, $C_{17}H_{19}N_3O_2$ requires C, 68.67; H, 6.44; N, 14.13%.) MS (EI): *m/z* 297 (M$^+$, 70%), IR(FT): 1770, 1690 (two CO). ^{1}H NMR; 1.2 (t, *J* = 9.8 Hz, 3H, C*H*$_3$–CH$_2$–), 1.6–2.0 (m, 10H, cyclohexyl), 3.2 (q, *J* = 9.8 Hz , 2H, CH$_3$–C*H*$_2$–), 7.2–8.1 (m, 4H, Ar–H).

5.3.2. For compound VIIb. It was separated as faint yellowish white crystals (70% yield), m.p. 90 °C. (Found: C, 73.19; H, 5.99; N, 11.35, $C_{22}H_{21}N_3O_2$ requires C, 73.52; H, 5.89; N, 11.69%.) MS (EI): *m/z* 359 (M$^+$, 22%), IR(FT): 1779, 1684 (two CO). ^{1}H NMR; 1.5–2.0 (m, 10H, cyclohexyl) 4.5–4.7 (m, 2H, C*H*$_2$–Ar), 7.2–8.1 (m, 9H, Ar–H).

5.3.3. For compound VIIc. It was separated as faint yellowish white crystals (87% yield), m.p. 150 °C. (Found: C, 61.12; H, 5.99; N, 12.98, $C_{17}H_{18}ClN_3O_2$ requires C,

61.54; H, 5.47; N, 12.66%.) MS (EI): m/z 331 (M$^+$, 100%), m/z 333 (M+2, 36.1%); IR(FT): 1760, 1676 (two CO). ^{1}H NMR; 1.2 (t, $J = 9.4$ Hz, 3H, CH_3–CH$_2$–), 1.4–2.0 (m, 10H, cyclohexyl), 3.21 (q, $J = 9.4$ Hz, 2H, CH$_3$–CH_2–), 7.4–8.1 (m, 8H, Ar–H).

5.3.4. For compound VIId.
It was separated as faint yellowish white crystals (68% yield), m.p. 240 °C. (Found: C, 67.98; H, 5.56; N, 10.22, $C_{22}H_{20}ClN_3O_2$ requires C, 67.09; H, 5.12; N, 10.67%.) MS (EI): m/z 393 (M$^+$, 43.9%), m/z 395(M+2, 14.8%); IR(FT): 1789, 1684 (two CO). ^{1}H NMR; 1.3–2.0 (m, 10H, cyclohexyl) 4.6–4.7 (m, 2H, CH^2–Ar), 7.1–8.1 (m, 8H, Ar–H).

5.4. Preparation of 2-acyl-3,3-pentamethylene-1,2,3,9-tetrahydro-imidazo[5,1-*b*]quinazoline-1,9-diones (VIIIa–d)

Method A: Compound (**VI**a) (0.269 g, 1 mmol) was refluxed with the appropriate acid anhydride [viz.: acetic anhydride, propionic anhydride] (0.3 mol) for 3 h. The reaction mixture was poured onto ice and the formed solid was filtered and the obtained precipitate was dried and crystallized from acetone–ether to give **VIII**a,b. *Method B*: To a mixture of benzoyl chloride (0.05 g, 0.33 mmol) in dry acetone (20 ml) and K$_2$CO$_3$ (3 g, 20 mmol) was added a solution of (**V**a,b) (0.33 mmol) in dry acetone (10 ml), and the mixture was refluxed for 24 h. The solvent was evaporated under vacuum and the residue was triturated with ether. The separated solid was filtered and crystallized from an acetone-ether mixture to produce **VIII**c,d.

5.4.1. For compound VIIIa.
It was separated as pale white crystals (67% yield), m.p. 170 °C. (Found: C, 65.95; H, 5.73; N, 13.82, $C_{17}H_{17}N_3O_3$ requires C, 65.58; H, 5.50; N, 13.50%.) MS (EI): m/z 311 (M$^+$, 18.4%); IR(FT): 1715, 1630, 1523 (three CO). ^{1}H NMR; 1.4–1.9 (m, 10H, cyclohexyl), 2.1 (s, 3H, CH_3–CO), 7.6–7.9 (m, 4H, Ar–H).

5.4.2. For compound VIIIb.
It was separated as pale white crystals (75% yield), m.p. 240 °C. (Found: C, 66.18; H, 6.09; N, 12.49, $C_{18}H_{19}N_3O_3$ requires C, 66.45; H, 5.89; N, 12.91%.) MS (EI): m/z 325 (M$^+$, 40%), IR(FT): 1716, 1606, 1523 (three CO). ^{1}H NMR; 1.01 (t, $J = 10.2$ Hz, 3H, CH_3–CH$_2$–CO), 1.3–1.9 (m, 10H, cyclohexyl), 2.1 (q, $J = 10.2$ Hz, 2H, CH$_3$–CH_2–CO), 7.6–7.9 (m, 4H, Ar–H).

5.4.3. For compound VIIIc.
It was separated as pale white crystals (78% yield), m.p. 190 °C. (Found: C, 70.98; H, 5.61; N, 10.99, $C_{22}H_{19}N_3O_3$ requires C, 70.76; H, 5.13; N, 11.25%.) MS (EI): m/z 373 (M$^+$, 23.8%); IR(FT): 1720.9, 1682, 1610 (three CO). ^{1}H NMR; 1.3–1.7 (m, 10H, cyclohexyl), 7.4–8.2 (m, 9H, Ar–H).

5.4.4. For compound VIIId.
It was separated as faint yellowish white crystals (75% yield), m.p. 180 °C. (Found: C, 65.15; H, 4.51; N, 10.83, $C_{22}H_{18}ClN_3O_3$ requires C, 64.79; H, 4.45; N, 10.3%.) MS (EI): m/z 407 (M$^+$, 100%), m/z 409 (M+2, 32.2%); IR(FT): 1785.9, 1659, 1602 (three CO). ^{1}H NMR; 1.4–1.9 (m, 10H, cyclohexyl), 7.6–8.3 (m, 8H, Ar–H).

5.5. Preparation of 2-[2-oxo-2-(4-arylpiperazin-1-yl)ethyl]-3,3-pentamethyl-ene-1,2,3,9-tetrahydro-imidazo[5,1-*b*]quinazoline-1,9-diones (IXa–g) and 2-(1-oxo-1-(4-arylpiperazin-1-yl)propan-2-yl)-3,3-pentamethylene-1,2,3,9-tetrahydro-imidazo[5,1-*b*]quinazoline-1,9-diones (IXh–i)

General procedure: To a mixture of (**VI**a,b) (1.8 mmol) and anhydrous K$_2$CO$_3$ (1 g) in dry acetone (30 ml), the appropriate 4-aryl-1-chloroacylpiperazines (**10**a–e) [viz.: 4-phenyl-1-(2-chloroacetyl)piperazine, 4-[(2-methoxy)phenyl]-1-(2-chloroacetyl)piperazine, 4-[(2-fluoro)phenyl]-1-(2-chloroacetyl)piperazine, 4-[(4-fluoro)phenyl]-1-(2-chloroacetyl)piperazine, and 4-phenyl-1-(2-chloro-1-propionyl)piperazine] (2.0 mmol) were added. The reaction mixture was refluxed for 24 h and then filtered, and the filtrate was evaporated under vacuum. The residue thus obtained was triturated with ether where a precipitate was formed. The solid precipitate was then washed with ether and crystallized from acetone–ether mixture to obtain the titled compounds (**IX**a–i).

5.5.1. For compound IXa.
It was separated as pale white crystals (75% yield), m.p. 130 °C. (Found: C, 68.01; H, 6.09; N, 15.17, $C_{27}H_{29}N_5O_3$ requires C, 68.77; H, 6.2; N, 14.85%.) MS (EI): m/z 471 (M$^+$, 29.2%); IR(FT): 1772, 1686, 1641 (three CO). ^{1}H NMR; 1.6–1.7 (m, 10H, cyclohexyl), 3.1–3.7 (t, (t, $J = 6.4$ Hz, 4H, piperazine N$_4$–(CH_2)$_2$), 3.6–3.7 (t, $J = 6.4$ Hz, 4H, piperazine N$_1$–(CH_2)$_2$), 5.0 (m, 2H, CO–CH_2–N); 7.2–7.8 (m, 9H, Ar–H).

5.5.2. For compound IXb.
It was separated as white crystals (78% yield), m.p. 150 °C. (Found: C, 61.32; H, 5.78; N, 13.96, $C_{27}H_{27}ClFN_5O_3$ requires C, 61.89; H, 5.19; N, 13.37%.) MS (EI): m/z 523 (M$^+$, 26.8%), m/z 525 (M+2, 7.91%); IR(FT): 1785, 1691, 1634 (three CO). ^{1}H NMR; 1.5–2.0 (m, 10H, cyclohexyl), 3.0–3.3 (t, $J = 6.8$ Hz, 4H, piperazine N$_4$–(CH_2)$_2$), 3.5–3.7 (t, $J = 6.8$ Hz, 4H, piperazine N$_1$–(CH_2)$_2$), 4.3–4.5 (m, 2H, CO–CH_2–N); 6.8–7.9 (m, 7H, Ar–H).

5.5.3. For compound IXc.
It was separated as tan crystals (78% yield), m.p. 120 °C. (Found: C, 67.12; H, 6.67; N, 13.46, $C_{28}H_{31}N_5O_4$ requires C, 67.05; H, 6.23; N, 13.96%.) MS (EI): m/z 501 (M$^+$, 17.5%); IR(FT): 1772, 1689, 1699 (three CO). ^{1}H NMR; 1.4–2.1 (m, 10H, cyclohexyl), 3.0–3.32 (t, $J = 6.6$ Hz, 4H, piperazine N$_4$–(CH_2)$_2$), 3.5–3.81 (t, $J = 6.6$ Hz, 4H, piperazine N$_1$–(CH_2)$_2$), 4.1 (s, 3H, OCH$_3$), 5.0–5.2 (m, 2H, CO–CH_2–N); 7.5–7.8 (m, 8H, Ar–H).

5.5.4. For compound IXd.
It was separated as pale white crystals (67% yield), m.p. 120 °C. (Found: C, 66.71; H, 5.23; N, 14.02, $C_{27}H_{28}FN_5O_3$ requires C, 66.24; H, 5.77; N, 14.31%.) MS (EI): m/z 489(M$^+$, 100%); IR(FT): 1771, 1690, 1650 (three CO). ^{1}H NMR; 1.5–2.0 (m, 10H, cyclohexyl), 3.0–3.30 (t, $J = 6.0$ Hz, 4H, piperazine N$_4$–(CH_2)$_2$), 3.5–3.7 (t, $J = 6.0$ Hz, 4H, piperazine N$_1$–(CH_2)$_2$), 4.3–4.5 (m, 2H, CO–CH_2–N); 6.8–7.9 (m, 8H, Ar–H).

5.5.5. For compound IXe.
It was separated as pale yellowish white crystals (80% yield), m.p. 150 °C. (Found: C, 63.65; H, 5.94; N, 13.73, $C_{27}H_{28}ClN_5O_3$ requires C,

64.00 H, 5.58; N, 13.81%.) MS (EI): *m/z* 505 (M$^+$, 19.8%), *m/z* 507 (M+2, 6.91%); IR(FT): 1772, 1618, 1641 (three CO). ^{1}H NMR; 1.5–1.9 (m, 10H, cyclohexyl), 3.0–3.40 (t, *J* = 6.0 Hz, 4H, piperazine N$_4$–(C*H*$_2$)$_2$), 3.5–3.7 (t, *J* = 6.0 Hz, 4H, piperazine N$_1$–(C*H*$_2$)$_2$), 4.3–4.6 (m, 2H, CO–C*H*$_2$–N); 6.7–7.8 (m, 8H, Ar–H).

5.5.6. For compound IXf. It was separated as tan crystals (77% yield), m.p. 120 °C. (Found: C, 60.90; H, 5.68; N, 13.99, C$_{27}$H$_{27}$ClFN$_5$O$_3$ requires C, 61.89 H, 5.19; N, 13.37%.) MS (EI): *m/z* 523 (M$^+$, 15.8%), *m/z* 525 (M+2, 5.0%); IR(FT): 1785, 1691, 1634 (three CO). ^{1}H NMR; 1.5–2.0 (m, 10H, cyclohexyl), 3.0–3.3 (t, *J* = 6.8 Hz, 4H, piperazine N$_4$–(C*H*$_2$)$_2$), 3.5–3.7 (t, *J* = 6.8 Hz, 4H, piperazine N$_1$–(C*H*$_2$)$_2$), 4.3–4.5 (m, 2H, CO–C*H*$_2$–N); 6.8–7.9 (m, 7H, Ar–H).

5.5.7. For compound IXg. It was separated as tan crystals (63% yield), m.p. 140 °C. (Found: C, 62.98; H, 6.12; N, 13.55, C$_{28}$H$_{30}$ClN$_5$O$_4$ requires C, 62.7, H, 5.6; N, 13.07%.) MS (EI): *m/z* 535 (M$^+$, 37.4%), *m/z* 537 (M+2, 14.8%); IR(FT): 1773, 1696, 1654 (three CO). ^{1}H NMR; 1.5–2.0 (m, 10H, cyclohexyl), 3.0–3.3 (t, *J* = 6.6 Hz, 4H, piperazine N$_4$–(C*H*$_2$)$_2$), 3.5–3.8 (t, *J* = 6.6 Hz, 4H, piperazine N$_1$–(C*H*$_2$)$_2$), 3.6 (s, 3H, OC*H*$_3$), 5.0 (m, 2H, CO–C*H*$_2$–N); 7.5–7.8 (m, 7H, Ar–H).

5.5.8. For compound IXh. It was separated as white crystals (74% yield), m.p. 150 °C. (Found: C, 69.71; H, 6.89; N, 14.29, C$_{28}$H$_{31}$N$_5$O$_3$ requires C, 69.26, H, 6.43; N, 14.42%.) MS (EI): *m/z* 485 (M$^+$, 6.0%); IR(FT): 1776, 1693, 1634 (three CO). ^{1}H NMR; 1.48 (d, *J* = 5.2 Hz, 3H, C*H*$_3$–CHCO), 1.6–1.9 (m, 10H, cyclohexyl), 3.0–3.43 (t, *J* = 6.6 Hz, 4H, piperazine N$_4$–(C*H*$_2$)$_2$), 3.5–3.61 (t, *J* = 6.6 Hz, 4H, piperazine N$_1$–(C*H*$_2$)$_2$), 4.7 (q, *J* = 5.2 Hz, 1H, CH$_3$–C*H*–CO); 6.8–7.8 (m, 9H, Ar–H).

5.5.9. For compound IXi. It was separated as white crystals (76% yield), m.p. 155 °C. (Found: C, 64.24; H, 6.09; N, 13.67, C$_{28}$H$_{30}$ClN$_5$O$_3$ requires C, 64.67, H, 5.81; N, 13.47%.) MS (EI): *m/z* 519 (M$^+$, 25.8%), *m/z* 521 (M+2, 8.7%); IR(FT): 1772, 1695, 1634 (three CO). ^{1}H NMR; 1.5 (d, *J* = 5.6 Hz, 3H, C*H*$_3$–CHCO), 1.55–1.8 (m, 10H, cyclohexyl), 3.2–3.43 (t, *J* = 6.8 Hz, 4H, piperazine N$_4$–(C*H*$_2$)$_2$), 3.4–3.7 (t, *J* = 6.8 Hz, 4H, piperazine N$_1$–(C*H*$_2$)$_2$), 4.7 (q, *J* = 5.6 Hz, 1H, CH$_3$–C*H*CO); 6.8–7.9 (m, 8H, Ar–H).

6. Pharmacological tests

In vivo biological evaluation of the effect of the tested compounds on the arterial blood pressure of normotensive adult cats, adopting the reported method,[34] which were previously used in our laboratory in a previous publications.[35]

6.1. Materials

Heparin (5000 IU/mL), phenobarbitone sodium (30 mg/kg), and clonidine HCl (0.15 mg/mL), Tested compounds are **VI**b, **VIII**a, **IX**a, **IX**b, **IX**c, **IX**e, and **IX**g (0.010–0.066 mg/kg).

6.2. Methods

Male cats weighing 2–3 kg were anaesthetized with phenobarbitone sodium (30 mg/kg ip) and the femoral artery of the leg was exposed and then connected to saline infusion through a cannula. Tested drugs were all dissolved in 1 mL DMSO and then diluted with water to the final volume. Tested compounds were injected gradually in increasing doses (0.01–0.66 mg/kg). The effects of prazosin (reference drug) and saline/DMSO (control) were compared those of the tested compounds. The results are given in Table 6.

6.3. Catalyst molecular modeling experiments

All molecular modeling work was performed on Silicon Graphic (SGI), Fuel workstation (500 MHz, R 14000 A^{TM} processor, 512 MB memory) using the Catalyst package of Molecular Simulation (version 4.8), under an IRIX 6.8 operating system, at Faculty of Pharmacy, Ain Shams University. A generalized visualizer, confirm, info, HipHop, Compare/fit, force field was used throughout.

Training sets were selected, as described in Section 1. Molecules were built within the catalyst and conformational models for each compound were generated automatically using the poling algorithm. This emphasizes representative coverage over a 20 kcal mol^{-1} energy range above the estimated global energy minimum and the best searching procedure was chosen. The training molecules with their associated conformational models were submitted to catalysis by using default common features hypothesis generation by using HipHop commands. The chemical function groups (features) used in this generation step included H-bond acceptor, hydrophobic groups, and positive ionizable groups. The selected ideal hypotheses were by matching with that of the literature and by consistency of fitting values of the respective ligands with the experimental results.

References and notes

1. Barbaro, R.; Betti, L.; Botta, M.; Corelli, F.; Giannaccini, G.; Maccari, L.; Manetti, F.; Strappaghetti, G.; Corsano, F. *J. Med. Chem.* **2001**, *44*, 2118–2132.
2. Bylund, D. B.; Eikenberg, D. C.; Heieble, J. P.; Langer, S. Z.; Lefkowiskitz, R. J.; Minneman, K. P.; Molinoff, P. B.; Rufolo, R. R.; Trendelenburg, U. *Pharmacol. Rev.* **1994**, *46*, 121.

3. Forray, C.; Wetzel, J. M.; Brancheck, T. A.; Bard, J. A.; Chin, G.; Shapiro, E.; Tang, R.; Lepor, H.; Hartig, P. R.; Weinshbank, R. I.; Gluchowski, C. *Mol. Pharmacol.* **1994**, *45*, 703.
4. Michael, A. P.; Ann, L. S.; Theodore, P. B.; Raymond, S. L.; Richard, W. R.; Jerry, D.; Carlos, F. *J. Med. Chem.* **1998**, *41*, 1206.
5. Croxatto, R.; Huidoobro, F. *Arch. Int. Pharmacodyn.* **1956**, *106*, 207.
6. Paton, W. D. M. *Proc. R. Soc. Lond* **1961**, *21*, 154.
7. Bremner, J. B.; Coban, B.; Griffith, R.; Greoenewoud, K. M.; Yates, B. F. *Bioorg. Med. Chem.* **2000**, *8*, 201–214.
8. Barbaro, R.; Betti, L.; Botta, M.; Corelli, F.; Giannaccini, G.; Maccari, L.; Manetti, F.; Strappaghetti, G.; Corsano, F. *J. Med. Chem.* **2002**, *45*, 3603.
9. Barbaro, R.; Betti, L.; Botta, M.; Corelli, F.; Giannaccini, G.; Maccari, L.; Manetti, F.; Strappaghetti, G.; Corsano, F. *Bioorg. Med. Chem.* **2002**, *10*, 361.
10. Guimares, S.; Daniel, M. *Pharmacol. Rev.* **2001**, *53*, 319–356.
11. Bremner, J. B.; Coban, B.; Griffith, R. *J. Comput.-Aided Mol. Des.* **1996**, *10*, 545.
12. Green, J.; Kahn, S.; Savoj, H.; Sprague, P.; Teig, S. *J. Chem. Inf. Comput. Sci.* **1994**, *34*, 1297.
13. Barnum, D.; Green, J.; Smellie, A.; Sprague, P. *J. Chem. Inf. Comput. Sci.* **1996**, *36*, 563.
14. Alex, A. C.; Jean, M. L.; Fabrice, L. G.; Yolande, H.; Lucile, V. L.; Jean, J. D.; Christine, C.; Michel, L. *J. Med. Chem.* **1997**, *40*, 2931.
15. Nazulak, J.; Vigouret, J. M.; Jaton, A. L.; Hofmann, A.; Dravid, A. R.; Weber, H. P.; Kalkman, H. O.; Walkinshow, M. D. *J. Med. Chem.* **1992**, *35*, 480.
16. De Marinis, R. M.; Hieble, J. P. *J. Med. Chem.* **1983**, *26*, 1215.
17. Petrus, J. P.; Isabelle, R.; Thierry, W. *J. Pharm. Exp. Ther.* **2003**, *305*, 1015.
18. Bostrom, J.; Norrby, P. O.; Liljefors, T. *J. Comput.-Aided Mol. Des.* **1998**, *12*, 283–396.
19. Pettersson, I.; Liljefores, T. *J. Comput.-Aided Mol. Des.* **1987**, *1*, 143–152.
20. Chern, J. W.; Shiau, C. Y.; Lu, G. Y. *Bioorg. Med. Chem. Lett.* **1991**, *1*, 571.
21. Chern, J. W.; Tao, P. L.; Yen, M. H.; Lu, G. Y.; Shiau, C. Y.; Lai, Y. J.; Chien, S. L.; Chan, C. H. *J. Med. Chem.* **1993**, *36*, 2196.
22. Jen, T.; Dienel, B.; Bowman, H.; Petta, J.; Helt, A.; Love, B. *J. Med. Chem.* **1972**, *15*, 727.
23. Russo, F.; Romeo, G.; Guccione, S.; Ambrosini, G.; De Blasi, A. *Eur. J. Med. Chem.* **1993**, *28*, 499.
24. Seki, N.; Nishiye, E.; Itoh, T. *Br. J. Pharmacol.* **1988**, *93*, 702.
25. Hess, H. G.; Cronin, T. H.; Scriabine, A. *J. Med. Chem.* **1968**, *11*, 130.
26. Campell, S. F.; Davey, M. J.; Lewis, B. N.; Palmer, M. J. *J. Med. Chem.* **1987**, *30*, 49.
27. Melchiorre, C.; Angeli, P.; Bolognesi, M. L.; Chiarini, A.; Giardina, D.; Gulini, U.; Leonardi, A.; Marucci, G.; Minarini, A.; Pigini, M.; Quaglia, W.; Rosini, M.; Tumiatti, V. *Pharm. Acta Helv.* **2000**, *74*, 181.
28. Carrington, H. C. *J. Am. Chem. Soc.* **1947**, *41*, 683.
29. Carrington, H. C. *J. Am. Chem. Soc.* **1947**, *41*, 684.
30. Carrington, H. C.; Waring, W. S. *J. Am. Chem. Soc.* **1950**, *40*, 356.
31. Costa, A.; Martignoni, E.; Blandini, F.; Petraglia, P.; Genazzam, A. R.; Nappi, G. *Clin. Neuropharmacol.* **1993**, *16*, 127–138.
32. Bonuso, S.; Di Stasio, E.; Marano, E.; Covelli, V.; Testa, N.; Tetto, A.; Buscaino, G. A. *Acia Neurol.* **1994**, *16*, 1–10.
33. Larsen, P. K.; Liljefors, T.; Madsen, U. *Textbook of Drug Design and Discovery*, 3rd ed, **2002**, pp 302–312.
34. John, H.; Robert, M.; Graham, S.; Dianne, M. P. *J. Biol. Chem.* **1995**, *270*, 23189.
35. Litchfield, J. T.; Wilcoxon, F. A. *J. Pharmacol. Exp. Ther.* **1949**, *96*, 99.
36. Ismail, M. A. H.; Abouzied, K. A. M.; Farag, A. E. *Alex J. Pharm. Sci.* **2002**, *14*, 151.